Graphical Synopsis

Special Issue: Final reports of DFG priority program 1415 Crystalline non-equilibrium phases Guest Editors: Wolfgang Bensch, Josef Breu

Editorial

Tobias Lüdtke, Dominik Weber, Alexander Schmidt, Alexander Müller, Christoph Reimann, Nils Becker, Thomas Bredow, Richard Dronskowski, Thorsten Ressler and Martin Lerch

Synthesis and characterization of metastable transition metal oxides and oxide nitrides

DOI 10.1515/zkri-2016-1961
Z. Kristallogr. 2017; 232(1–3): 3–14

Synopsis: New routes to metastable vanadium sesquioxide and tantalum oxide nitride (γ- and δ-phase) are presented. The present results are compared to experimental data and to previous calculations at hybrid DFT level.

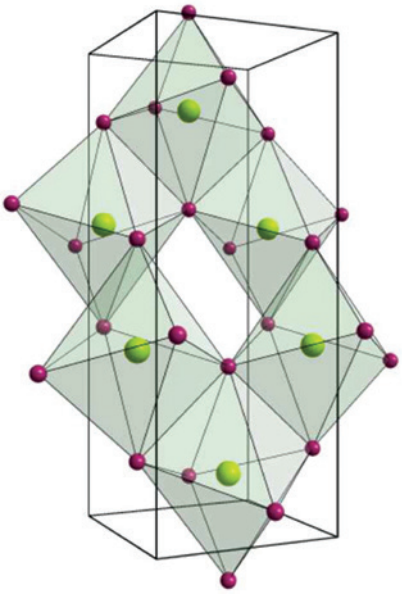

Thi Yen Nguyen, Ernst A. Roessler, Klaus Rademann and Franziska Emmerling

Control of organic polymorph formation: crystallization pathways in acoustically levitated droplets

DOI 10.1515/zkri-2016-1964
Z. Kristallogr. 2017; 232(1–3): 15–24

Synopsis: The homogeneous crystallization of paracetamol from solution and in an acoustic levitator indicates the influence of the solvents' properties and the initial concentrations on the crystallization pathways, the appearing intermediates and the resulting products.

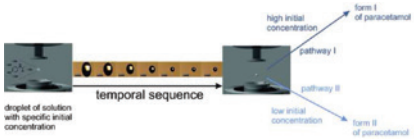

Peter Zietlow, Tobias Beirau, Boriana Mihailova, Lee A. Groat, Thomas Chudy, Anna Shelyug, Alexandra Navrotsky, Rodney C. Ewing, Jochen Schlüter, Radek Škoda and Ulrich Bismayer

Thermal annealing of natural, radiation-damaged pyrochlore

DOI 10.1515/zkri-2016-1965
Z. Kristallogr. 2017; 232(1–3): 25–38

Synopsis: The effect of thermal annealing (400–1000 K) on radiation-damaged pyrochlores has been investigated by Raman scattering, X-ray powder diffraction (XRD), and combined differential scanning calorimetry/thermogravimetry (DSC/TG). This study revealed a correlation between the initial structural damage state and the recrystallization of metamict natural pyrochlore. Considerable differences occur during thermally-induced recrystallization depending on the degree of damage.

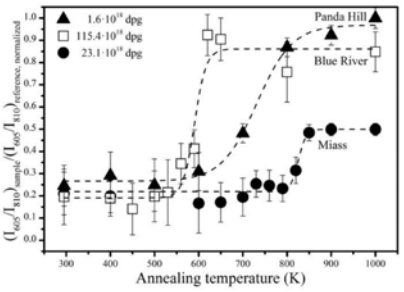

Andreas Schiener, Ella Schmidt, Christoph Bergmann, Soenke Seifert, Dirk Zahn, Alexander Krach, Richard Weihrich and Andreas Magerl

The formation of CdS quantum dots and Au nanoparticles

DOI 10.1515/zkri-2016-1978
Z. Kristallogr. 2017; 232(1–3): 39–46

Synopsis: Mean particle radius as a function of reaction time for the lognormal distributed spherical Au nanoparticles.

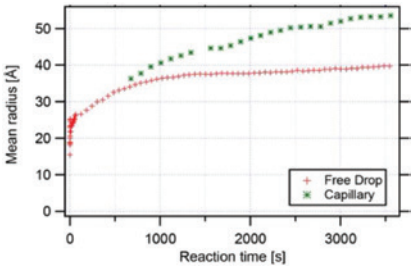

Günther Thiele, Silke Santner and Stefanie Dehnen

Crystalline chalcogenido metalates – synthetic approaches for materials synthesis and transformation

DOI 10.1515/zkri-2016-1976
Z. Kristallogr. 2017; 232(1–3): 47–54

Synopsis: On the example of our recent results we discuss and compare the formation and transformation of metalate compounds under solvothermal, ionothermal and solution based reaction conditions.

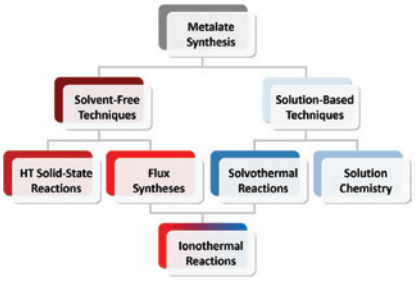

Thomas Martin, Paul Niemietz, Dominik Greim, Philipp Ectors, Jürgen Senker, Dirk Zahn and Josef Breu

Fundamental theoretical and practical investigations of the polymorph formation of small amphiphilic molecules, their co-crystals and salts

DOI 10.1515/zkri-2016-1977
Z. Kristallogr. 2017; 232(1–3): 55–67

Synopsis: The amphiphilic nature of benzoic acid, benzoates and benzamide, gives rise to an unexpected rich polymorphism. In combination with rather rigid and small molecular structures these compounds are ideal model systems for a systematic and concerted investigation of molecular polymorphism.

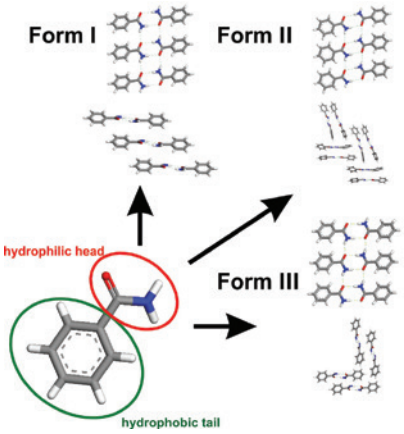

Nils Becker, Christoph Reimann, Dominik Weber, Tobias Lüdtke, Martin Lerch, Thomas Bredow and Richard Dronskowski

A density-functional theory approach to the existence and stability of molybdenum and tungsten sesquioxide polymorphs

DOI 10.1515/zkri-2016-1960
Z. Kristallogr. 2017; 232(1–3): 69–75

Synopsis: The sesquioxides of molybdenum and tungsten are systematically predicted *ab initio* including suggestions for their synthesis and crystal structures. Both Mo_2O_3 and W_2O_3 will form stable corundum structures at high pressures, the reaction pressure being 15 GPa for Mo_2O_3 and over 60 GPa for W_2O_3.

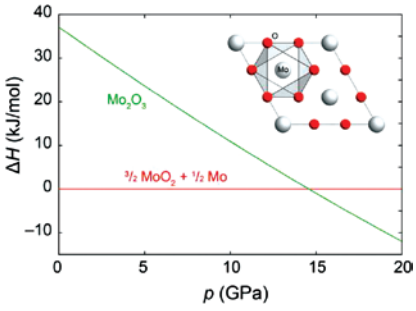

Sergej Springer, Niclas Heidenreich, Norbert Stock, Leo van Wüllen, Klaus Huber, Stefano Leoni and Michael Wiebcke

The ZIF system zinc(II) 4,5-dichoroimidazolate: theoretical and experimental investigations of the polymorphism and crystallization mechanisms

DOI 10.1515/zkri-2016-1968
Z. Kristallogr. 2017; 232(1–3): 77–90

Synopsis: In line with theoretical predictions of a great *static* conformational variety of the [Zn(4,5-dichloroimidazolate)2]-SOD framework, we have been able to realize two SOD-type materials. *In-situ* scattering experiments have provided insights into the mechanisms of crystallization.

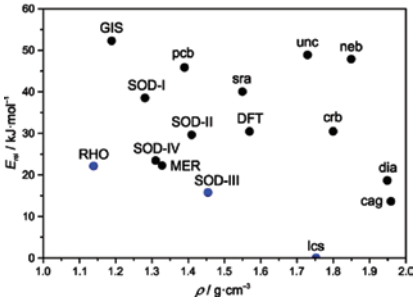

Michael Schöneich, Andrea Hohmann, Peer Schmidt, Florian Pielnhofer, Frederik Bachhuber, Richard Weihrich, Oliver Osters, Marianne Köpf and Tom Nilges

Element allotropes and polyanion compounds of pnicogenes and chalcogenes: stability, mechanisms of formation, controlled synthesis and characterization

DOI 10.1515/zkri-2016-1966
Z. Kristallogr. 2017; 232(1–3): 91–105

Synopsis: Element and polyanionic compounds and structures of pnicogen and chalcogen elements are investigated with respect phase formation, stability and structures from combined experimental and theoretical methods within the EnPhaSyn concept.

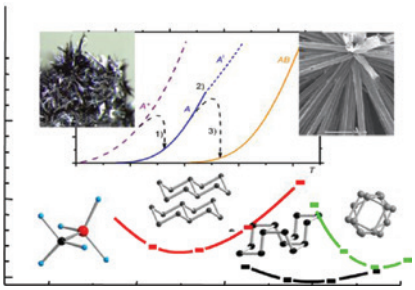

Martin Wilkening, Andre Düvel, Florian Preishuber-Pflügl, Klebson da Silva, Stefan Breuer, Vladimir Šepelák and Paul Heitjans

Structure and ion dynamics of mechanosynthesized oxides and fluorides

DOI 10.1515/zkri-2016-1963
Z. Kristallogr. 2017; 232(1–3): 107–127

Synopsis: High-energy ball milling offers the possibility to prepare ceramic materials being characterized by non-equilibrium local structures. While conventional routes often yield thermodynamically stable compounds, mechanosynthesis is able to provide direct access to metastable, novel phases through a facile and efficient one-step approach.

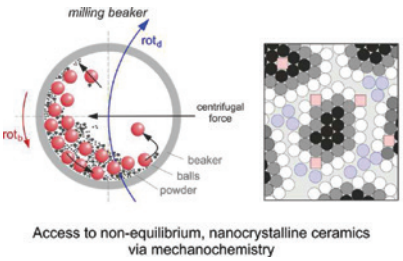

Lukas Schlicker, Maged F. Bekheet and Aleksander Gurlo

Scaled-up solvothermal synthesis of nanosized metastable indium oxyhydroxide (InOOH) and corundum-type rhombohedral indium oxide (rh-In_2O_3)

DOI 10.1515/zkri-2016-1967
Z. Kristallogr. 2017; 232(1–3): 129–140

Synopsis: Phase pure metastable indium oxyhydroxide (InOOH) was synthesized in a nonaqueous solvothermal synthesis route in ethanol. T-pH maps summarize the impact of synthesis temperature and pH. Phase-pure InOOH was obtained in water-free solutions at mild temperatures (150–180 °C) in highly basic conditions (pH > 12). Calcination of InOOH at 375–700 °C in ambient air atmosphere results in metastable rhombohedral indium oxide (rh-In_2O_3). The synthesis protocol for InOOH material was sussecfully upscaled to batches of ca. 3 g with 78 % yield. The upscaled InOOH and rh-In_2O_3 specimens are available for further functional properties characterization.

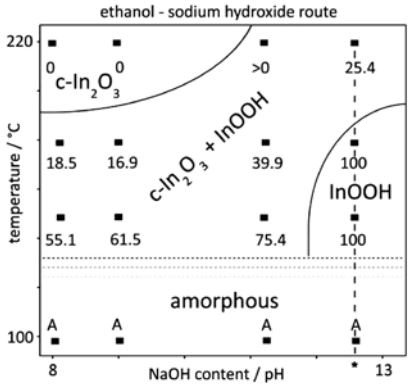

Leo van Wüllen, Jan Gerrit Schiffmann, Jakob Kopp, Zhongqing Liu, Holger Kirchhain, Andre Düvel and Paul Heitjans

Development and application of novel NMR methodologies for the in situ characterization of crystallization processes of metastable crystalline materials

DOI 10.1515/zkri-2016-1975
Z. Kristallogr. 2017; 232(1–3): 141–159

Synopsis: The development of a NMR methodology, which enables an analysis of local structural motifs on short (1–2 Å) and extended (2–6 Å) length scales without the need for fast magic angle spinning is reported. This approach will eliminate any possible interference between the enormous centripetal forces which occur during fast sample rotation (up to 10^7 g) and the chemical or physical process being monitored.

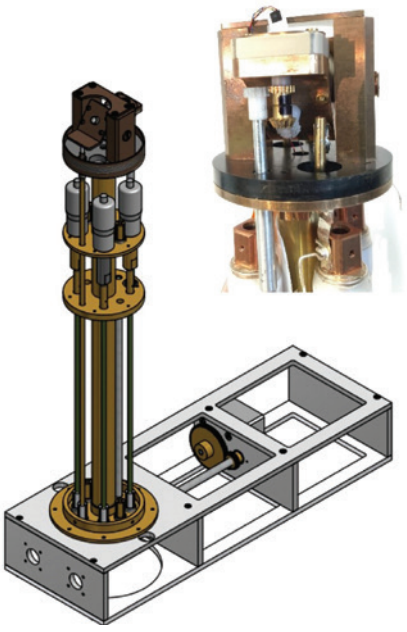

Ralph A. Henning, Thomas Leichtweiss, Daniel Dorow-Gerspach, Rüdiger Schmidt, Niklas Wolff, Ulrich Schürmann, Yannic Decker, Lorenz Kienle, Matthias Wuttig and Jürgen Janek

Phase formation and stability in TiO_x and ZrO_x thin films: Extremely substoichiometric functional oxides for electrical and TCO applications

DOI 10.1515/zkri-2016-1981
Z. Kristallogr. 2017; 232(1–3): 161–183

Synopsis: After the gas phase deposition an amorphous and non-stoichiometric precursor phase is deposited with a high Gibbs energy (bold curve). By annealing of such a thin film, a decomposition/disproportionation reaction proceeds (route from amorphous to ε, γ) until the thermodynamically stable phases (α, β) are obtained.

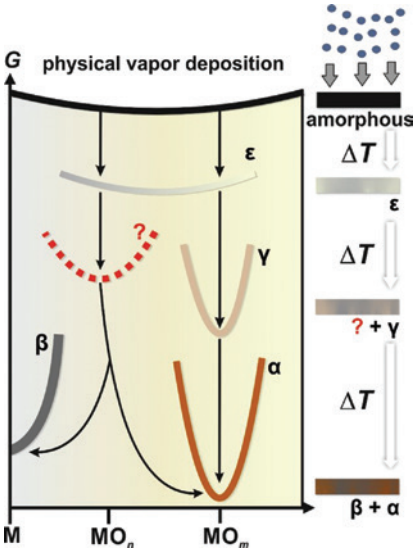

Marcus Weber, Maik Schlesinger, Markus Walther, Dirk Zahn, Christoph A. Schalley and Michael Mehring

Investigations on the growth of bismuth oxido clusters and the nucleation to give metastable bismuth oxide modifications

DOI 10.1515/zkri-2016-1970
Z. Kristallogr. 2017; 232(1–3): 185–207

Synopsis: The nucleation and growth of bismuth oxido clusters and metastable bismuth(III) oxide polymorphs were analyzed using analytical techniques such as ESI-MS, PXRD, X-ray single crystal structure analysis, X-ray scattering (PDF) accompanied by MD simulations. Polynuclear bismuth oxido clusters such as $[Bi_6O_4(OH)_4(NO_3)_5(H_2O)](NO_3)$ and $[Bi_{38}O_{45}(NO_3)_{20}(DMSO)_{28}](NO_3)_4 \cdot 4DMSO$ are the result of hydrolysis and reorganization processes starting from bismuth(III) nitrate in solution. The resulting cluster size depends strongly on the solvent used and they all contain the same central bismuth-oxygen building unit $\{Bi_6O_8\}$, which is a very stable structural arrangement. The polynuclear bismuth oxido clusters are preorganized precursors for the synthesis of metastable bismuth(III) oxide polymorphs such as β-Bi_2O_3.

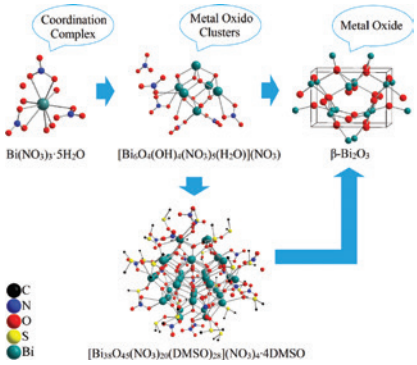

Manuel Wilke, Sven Bach, Tatiana E. Gorelik, Ute Kolb, Wolfgang Tremel and Franziska Emmerling

Divalent metal phosphonates – new aspects for syntheses, *in situ* characterization and structure solution

DOI 10.1515/zkri-2016-1971
Z. Kristallogr. 2017; 232(1–3): 209–222

Synopsis: Metal phosphonates offer an interesting opportunity for the design of multifunctional materials. A short review on the class of divalent metal phosphonates discussing their syntheses, structures, and applications is given. The advantages of the recently introduced mechanochemical pathway for the synthesis of divalent phosphonates are presented as a possibility to generate new, in certain cases metastable compounds. The benefits of *in situ* investigation of synthesis mechanisms as well as the implementation of sophisticated methods for the structure analysis of the resulting compounds are discussed.

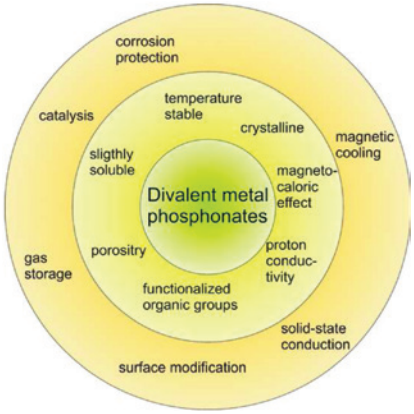

Bodo Böhme, Matej Bobnar, Alim Ormeci, Sarah Peters, Walter Schnelle, Michael Baitinger and Yuri Grin

Type-I silicon clathrates containing lithium

DOI 10.1515/zkri-2016-1983
Z. Kristallogr. 2017; 232(1–3): 223–233

Synopsis: The intermetallic phase $[Li_xBa_{8-x}][Li_ySi_{46-y}]$ is the first example of a clathrate-I silicide containing lithium. Li atoms occupy both cage and framework positions.

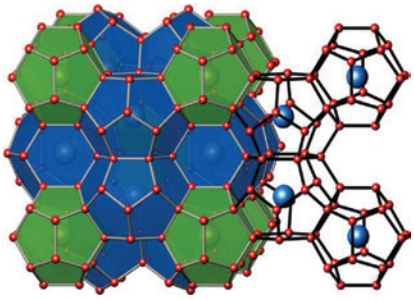

Matthias Regus, Svitlana Polesya, Gerhard Kuhn, Sergiy Mankovsky, Sage R. Bauers, David C. Johnson, Hubert Ebert and Wolfgang Bensch

Experimental and theoretical investigation of the chromium–vanadium–antimony system

DOI 10.1515/zkri-2016-1979
Z. Kristallogr. 2017; 232(1–3): 235–244

Synopsis: Simultaneous crystallization of hexagonal MSb and cubic M_3Sb (M = Cr, V) in ternary thin film sample.

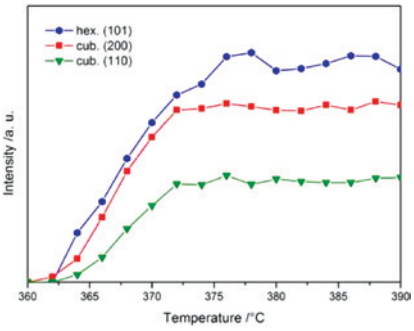

Martin Albat, Andrew Kentaro Inge and Norbert Stock

Synthesis and crystal structure of three new bismuth(III) arylsulfonatocarboxylates

DOI 10.1515/zkri-2016-1980
Z. Kristallogr. 2017; 232(1–3): 245–253

Synopsis: Solvothermal synthesis and structure elucidation of three new bismuth arylsulfonatocarboxylates is reported. In comparison to other known bismuth sulfonatocarboxylates their crystal structures are denser and contain higher condensed Bi–O units, which is due to the harsher reaction conditions employed. The structural trend is also reflected in the different coordination modes of the sulfonate and the carboxylate groups in the three title compounds, which have been summarized using the Harris notation.

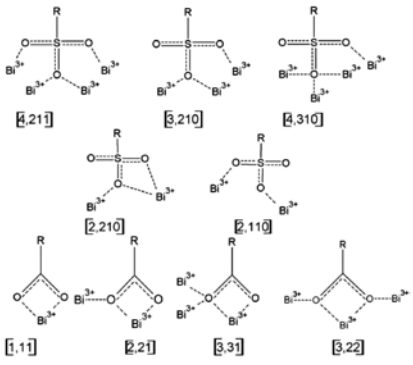

Michael Dietzsch, Iryna Andrusenko, Robert Branscheid, Franziska Emmerling, Ute Kolb and Wolfgang Tremel

Snapshots of calcium carbonate formation – a step by step analysis

DOI 10.1515/zkri-2016-1973
Z. Kristallogr. 2017; 232(1–3): 255–265

Synopsis: $CaCO_3$ formation by hydrolysis of carbonate ester hydrolysis was monitored by dynamic light scattering (DLS) and transmission electron microscopy (TEM). Homogeneous nucleation in solution led to the formation of amorphous calcium carbonate particles, which transformed *via* vaterite to calcite by dissolution and recrystallization. In the presence of Napolymethacrylate (Na-PMA), heterogeneous nucleation was suppressed and Ca-polymer aggregates were formed in the prenucleation stage. In the postnucleation stage, the presence of the polymer led to the formation of extended liquid-like networks.

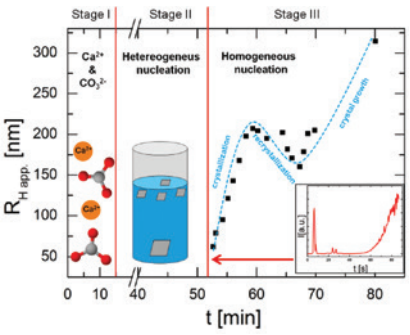

Formulae Index